Science of the Total Environment 450–451 (2013) 72–82

Contents lists available at SciVerse ScienceDirect

Science of the Total Environment

journal homepage: www.elsevier.com/locate/scitotenv

Assessment of climate change impacts on hydrology and water quality with a watershed modeling approach

Yuzhou Luo [a,*], Darren L. Ficklin [b], Xiaomang Liu [a,c], Minghua Zhang [a,*]

[a] Department of Land, Air, and Water Resources, University of California, Davis, CA, USA
[b] Department of Geography, Indiana University, Bloomington, Indiana, USA
[c] Institute of Geographic Sciences and Natural Resources Research, Chinese Academy of Sciences, Beijing, China

HIGHLIGHTS

- SWAT was modified by incorporating CO_2 impacts and stream temperature prediction.
- Updated SWAT was applied to watersheds in California under climate change scenarios.
- Evapotranspiration response to CO_2 concentration varied with vegetation type.
- Unfavorable conditions for cold-water species were predicted for future California.

ARTICLE INFO

Article history:
Received 20 November 2012
Received in revised form 19 January 2013
Accepted 1 February 2013
Available online 1 March 2013

Keywords:
Climate change
Hydrologic simulation
Stream temperature
SWAT
Watershed

ABSTRACT

The assessment of hydrologic responses to climate change is required in watershed management and planning to protect water resources and environmental quality. This study is designed to evaluate and enhance watershed modeling approach in characterizing climate change impacts on water supply and ecosystem stressors. Soil and Water Assessment Tool (SWAT) was selected as a base model, and improved for the CO_2 dependence of potential evapotranspiration and stream temperature prediction. The updated model was applied to quantify the impacts of projected 21st century climate change in the northern Coastal Ranges and western Sierra Nevada, which are important water source areas and aquatic habitats of California. Evapotranspiration response to CO_2 concentration varied with vegetation type. For the forest-dominated watersheds in this study, only moderate (1–3%) reductions on evapotranspiration were predicted by solely elevating CO_2 concentration under emission scenarios A2 and B1. Modeling results suggested increases in annual average stream temperature proportional to the projected increases in air temperature. Although no temporal trend was confirmed for annual precipitation in California, increases of precipitation and streamflow during winter months and decreases in summers were predicted. Decreased streamflow during summertime, together with the higher projected air temperature in summer than in winter, would increase stream temperature during those months and result in unfavorable conditions for cold-water species. Compared to the present-day conditions, 30–60 more days per year were predicted with average stream temperature > 20 °C during 2090s. Overall, the hydrologic cycle and water quality of headwater drainage basins of California, especially their seasonality, are very sensitive to projected climate change.

1. Introduction

Effects of climate change on the hydrologic cycle and water quality of a watershed are associated with large uncertainty from both the climate projections and the hydrologic modeling approaches. The interaction between climatic variables and hydrologic components involves multiple competing processes. For example, elevated concentration of atmospheric CO_2 has direct impacts on plant transpiration, which further alters the magnitude and seasonality of hydrologic components in the watershed. Studies indicated reduction of leaf stomatal conductance under high CO_2 concentration, suggesting a decrease of potential evapotranspiration (PET) (Medlyn et al., 2001; Morison, 1987; Wand et al., 1999). Conversely, there are evidences of positive relationship between CO_2 concentration and the total leaf area of a plant, i.e., elevated CO_2 concentration may also increase PET (Pritchard et al., 1999; Wand et al., 1999). In addition, CO_2 concentration also influences the rate of biomass production and thus shifts the plant growth pattern (Neitsch et al., 2011; Stockle et al., 1992). Therefore, the actual effects of elevated CO_2 concentration should be determined with consideration of local weather conditions. Similarly, in addition to its direct effects on stream temperature, higher air temperature is expected to increase PET and potentially decrease water yield to rivers, which further degrades the river water quality due to less dilution. However, global warming

* Corresponding authors. Tel.: +1 530 754 2447; fax: +1 530 752 5262.
E-mail addresses: yzluo@ucdavis.edu (Y. Luo), mhzhang@ucdavis.edu (M. Zhang).

0048-9697/$ – see front matter © 2013 Elsevier B.V. All rights reserved.
http://dx.doi.org/10.1016/j.scitotenv.2013.02.004

may also intensify hydrologic cycle and further lead to streamflow increase (Labat et al., 2004). While General Circulation Models (GCMs) together with greenhouse gas emission scenarios generate future climate data virtually for any place of the world, their implications for regional hydrologic cycle and environmental quality are yet poorly understood.

Watershed modeling approach has been widely used in translating the GCM-generated climate data to their potential effects and management implications on regional water resources. For example, modeling results of a lumped rainfall-runoff model (HSAMI) on the St. Lawrence tributaries, Canada, suggested higher winter discharges under climate change, which may induce important modifications of river hydrology and geomorphological processes to riparian ecosystem (Boyer et al., 2010). The Hydrologic Modeling System (HEC-HMS) was applied to the Siurana catchment, Spain, and indicated that the effects of climatic variables on future water resources was highly dependent on local soil moisture conditions (Candela et al., 2012). Climate sensitivity analysis for a hypothesized watershed in western Turkey was conducted based on Hydrological Simulation Program—Fortran (HSPF), and the authors concluded that seasonal variations of precipitation and temperature were very important in predicting the future response of watersheds (Göncü and Albek, 2010). More modeling efforts are based on the Soil and Water Assessment Tool (SWAT) with its built-in options for climate change studies. More than 80 papers have been published for SWAT applications under climate change scenarios for watersheds all around the world (https://www.card.iastate.edu/swat_articles/). SWAT is selected in this study as a base model to represent the climate change effects on hydrology and water quality simulations.

Streamflow and stream temperature are usually considered as representative variables in watershed management and planning. Streamflow is a comprehensive indicator of water resources and hydrologic processes in the drainage area. By relating to its components of surface runoff, lateral flow, and groundwater recharge, streamflow is also an important predictor variable for soil erosion and generation of other pollutants. In addition to physically based modeling of surface water quality, streamflow could be directly related to pollutant loadings in a river (Cohn, 1995; Runkel et al., 2004). Stream temperature itself is frequently included as one of the most important water quality indicators in surface water assessment such as the 303(d) listing by U.S Environmental Protection Agency (USEPA, 2011). It also has significant effects on in-stream biogeochemical variables/processes including algal growth, dissolved oxygen concentration, nutrient cycling and productivity, and chemical reaction kinetics (Ducharne, 2008; Mohseni et al., 2003; Ozaki et al., 2003). In addition, streamflow and stream temperature are major aspects of water quality for aquatic ecosystems, and affects the speciation and distribution of fish and other organisms. Reduced streamflow and/or higher stream temperature by human activity or climate change are related to the loss of formerly suitable habitats for native species (Dowling and Wiley, 1986; Harvey et al., 2006; Ligon et al., 1999; McCullough, 1999). Recently, there have been substantial research interests in assessing the impacts of projected climatic changes on stream temperatures and aquatic ecosystems (Ficklin et al., 2012a; Isaak et al., 2010, 2012; van Vliet et al., 2011; Webb et al., 2008). The determination of streamflow and stream temperature is therefore critical for the effective protection of water resources and water quality and the implementation of watershed management practices.

Two major issues have been identified for SWAT applications under climate change scenarios. First, the original SWAT inadequately represents the effects of CO_2 concentration on plant growth and associated transpiration estimation. The response of leaf stomatal conductance to the doubling of CO_2 concentration is described in SWAT with a reduction of 40% for all vegetation species, while the CO_2-induced increase of the maximum leaf area index (LAI) is not considered. In addition, only one value of CO_2 concentration is allowed for each set of SWAT simulation, limiting the model applications for continuous GCM data. Secondly, SWAT predicts stream temperature based on a simple linear relationship between air-water temperatures, which may not general reliable results for all watersheds. Efforts have been made to improve SWAT for some of the above issues (Eckhardt and Ulbrich, 2003; Ficklin et al., 2012a; Wu et al., 2012), but an integrated solution is not presented yet.

This study aims to update the original SWAT with more mechanistic responses of hydrologic components and stream temperature to climate change. In specific, (1) mathematic formulations are modified or added to SWAT to allow plant type-specific parameters in simulating the changes of stomatal conductance and leaf area index under elevated CO_2 level; (2) a hydroclimatological model for stream temperature prediction is developed and integrated into SWAT. The update SWAT model was applied to selected headwater drainage basins throughout California with historical weather condition (2001-2010) and downscaled GCM data (2001-2099). Results were analyzed for the model performance of streamflow and stream temperature, and their sensitivity to climatic variables.

2. Methods and materials

2.1. Soil and water assessment tool and its representations of changing climate

SWAT is a conceptual semi-distributed model developed by the United States Department of Agriculture (USDA) for watershed hydrology and water-quality operating on daily time step (Neitsch et al., 2011). In the model, the watershed of interest is divided into explicitly parameterized smaller areas of subbasins and enclosed hydrologic response units (HRUs). The HRUs are delineated by overlaying topography, soil, and land use maps, and assumed to be homogeneous with respect to their hydrologic properties. SWAT simulations can be separated into two major divisions of "land phase" for water and pollutant loadings to channels, and "routing phase" for in-stream water quantity and quality. A full description of SWAT can be found in Neitsch et al. (2011).

SWAT requires daily weather data as inputs. Climate change scenarios for precipitation, air temperature, and wind speed, therefore, can be easily reflected by manipulating the weather input files. In addition, SWAT allows user-defined monthly adjustments on precipitation, temperature, solar radiation, and humidity for each subbasin (input parameters of RFINC, TMPINC, RADINC, respectively, in the "sub" input files). In SWAT, CO_2 concentration can be also specified for each subbasin. CO_2 concentration is mainly used by SWAT to adjust the calculations of potential evapotranspiration and the biomass production. The effects of elevated CO_2 level on PET estimation will be discussed in the next section. For biomass production, SWAT adjusts radiation-use efficiency (RUE, kg/ha/[MJ/m^2]) for elevated atmospheric CO_2 concentrations (Stockle et al., 1992),

$$RUE = \frac{100CO_2}{CO_2 + \exp(r_1 - r_2 \cdot CO_2)} \quad (1)$$

where CO_2 (ppm) is the atmospheric CO_2 concentration, and r_1 and r_2 (dimensionless) are shape coefficients derived from two known RUE values at the reference CO_2 concentration (330 ppm) and a higher concentration provided in the SWAT built-in crop database ("crop.dat").

2.2. Modifications on SWAT for climate change study

2.2.1. CO_2 effects on PET estimation

Two competing processes are involved for the effects of elevated CO_2 level on evapotranspiration (ET) from vegetation. With higher CO_2 concentration, less stomata opening is required to obtain the amount of CO_2 necessary for photosynthesis and reduce transpiration rate. At the same time, plant growth is stimulated by higher CO_2 concentration with increased apparent quantum yield of photosynthesis, resulting in higher maximum leaf area index (LAI) and transpiration.

SWAT represents the CO_2-dependence of stomatal conductance in the Penman–Monteith method. In other two methods, the Priestley–Taylor method and the Hargreaves method, CO_2 effects on PET are not incorporated. For CO_2 concentration higher than the reference level (330 ppm), the maximum stomatal conductance (g) is modified as,

$$g_{CO_2} = g \cdot [1.4 - 0.4 \cdot (CO_2/330)] \quad (2)$$

where g and g_{CO2} (m/s) are the stomatal conductance at reference and given CO_2 concentrations, respectively. This equation implies that a doubling of CO_2 concentration from 330 ppm results in a 40% reduction in stomatal conductance (Easterling et al., 1992; Morison, 1987; Morison and Gifford, 1983). More recent studies indicated that Eq. (2) is only appropriate for arable land, while less reductions of stomatal conductance under elevated CO_2 are suggested for forest and range land. For example, Field et al. (1995) reported an average reduction of stomatal conductance of 23% by doubling CO_2 concentration based on 23 tree species. Similarly, 21% average reduction was reported for tree species, ranging from 8% for coniferous to 24% for deciduous (Medlyn et al., 2001). Generally, SWAT overestimates the reduction of stomatal conductance under elevated CO_2 concentration in watersheds with landuse types other than arable land. To incorporate the broad range of stomatal conductance responses of difference vegetation species, Eq. (2) was modified as,

$$g_{CO_2} = g \cdot [(1-c) + c \cdot (CO_2/330)] \quad (3)$$

where c (dimensionless) is the plant-specific factor of stomatal conductance in response to the doubling of CO_2 concentration. Negative values of c indicate the reduction of stomatal conductance. Based on the previous literature reviews, values of c used in this study were compiled in Table 1.

The original SWAT does not consider the effects of CO_2-simulated plant growth on PET, which can be formulated by following the same mathematic form as in Eq. (3),

$$LAI_{mx,CO_2} = LAI_{mx} \cdot [(1+l) - l \cdot (CO_2/330)] \quad (4)$$

where LAI_{mx} and $LAI_{mx,}CO_2$ (dimensionless) are the maximum LAI before and after the modification to reflect CO_2 effects, respectively, and l (dimensionless) is the vegetation-specific factor of LAI_{mx} to a doubled atmospheric CO_2 concentrations from the reference level of 330 ppm. Generally, crop species have greatest value of l, followed by trees and wild, non-woody species. Table 1 summarizes the values of l reported in the literature.

The original SWAT only allows a fixed value of atmospheric CO_2 concentration through the simulation period. Previous studies on CO_2 effects were generally conducted with paired simulations for the reference and updated CO_2 concentrations, implying an abrupt change. In this study, SWAT was modified to accept annually varied CO_2 concentrations specified in an additional input file. The impacts of elevated CO_2 on PET calculation were considered previously in customized modifications on early versions of SWAT (Eckhardt and Ulbrich, 2003; Wu et al., 2012). This study presents the first incorporation of those effects in the latest SWAT model. In addition, the coefficients c and l in this study were summarized with the specific crop codes as used in SWAT (Table 1), which would be helpful in the model applications especially with automated landscape characterizations.

2.2.2. Stream temperature simulation

In the original SWAT, stream temperature is simulated by a linear relationship to daily air temperature. The relationship was developed by regression analysis based on daily and weekly measurements from 11 streams in the Midwestern United States (Stefan and Preud'homme, 1993),

$$T_w = 5.0 + 0.75 T_{air} \quad (5)$$

where T_w and T_{air} (°C) are the stream temperature and air temperature, respectively, on the same day of simulation. Resulting stream temperature is assigned to both the water yield (total water flow of surface runoff, lateral flow and groundwater recharge) and the stream discharge in each subbasin.

A new model of stream temperature prediction is developed based on our previous study (Ficklin et al., 2012a). The new model simulates two major processes of water temperature: heat sources (or local contribution) at each subbasin and heat exchange in stream network. Hydrologic components of water flows including surface runoff, lateral flow, groundwater recharge, and streamflow are required in simulating stream temperature. For stream temperature simulation at subbasin level, therefore, a flow-weighted water temperature is calculated for the local contribution,

$$T_{w,local} = \frac{\sum_i \left(T_{w,i} Q_i\right)}{\sum_i Q_i} \quad (6)$$

where Q_i (m^3/d) are components of water yield from a subbasin (specifically, $i=1$ for snowmelt contribution to surface runoff, 2 for groundwater recharge, and 3 for other components of the total water yield including surface runoff and lateral flow contributed from rainfall), and $T_{w,i}$ (°C) is the corresponding temperature of the individual hydrologic component. The temperature is set to 0.1 °C for snowmelt and a user-defined annual groundwater temperature for groundwater flow. The concept of hypothesized equilibrium temperature ($T_{w,eq}$, °C) in some stream temperature models (Edinger et al., 1968; Mohseni and Stefan, 1999) was introduced to estimate the temperature for Q_3,

$$T_{w,3} = T_{w,eq} = \begin{cases} \lambda \cdot T_{air,lag} & T_{air,lag} > \varepsilon \\ 0.5\left(T_{air,lag} + \varepsilon\right) & T_{air,lag} \le \varepsilon \end{cases} \quad (7)$$

Table 1
Assumed responses in maximum stomatal conductance and maximum leaf area index to a doubled atmospheric CO_2 concentration.

Vegetation type	Typical landuse codes in SWAT	% change of stomatal conductance (c*100)	% change of maximum leaf area index (l*100)
Original SWAT			
All types	All types	−40 [1]	0
Updated SWAT in this study			
Deciduous forest	FRSD	−24 [2]	+7 [6]
Coniferous forest	FRSE	−8 [2]	+7 [6]
Mixed forest	FRST	−16 [3]	+7 [6]
Pasture	PAST	−26.5 [4]	+20 [4]
Range land	RNGE, RNGB	−20 [5]	+15 [5]
Arable land	AGRL, ORCD	−40 [1]	+37 [6]

Note: percent changes of stomatal conductance and maximum leaf area index are defined based on a doubled CO_2 concentration.
References: [1] (Morison, 1987), [2] (Medlyn et al., 2001), [3] the mean value of −24% (deciduous) and −8% (coniferous), [4] (Wand et al., 1999), the mean value of C3 and C4 grasses, [5] the median value between pasture and forest (Eckhardt and Ulbrich, 2003), [6] (Pritchard et al., 1999).

where $T_{air,lag}$ (°C) is the average of antecedent air temperature during the past *lag* days. Time lags are required in the regression analysis with a short (e.g., daily) time scale (Mohseni and Stefan, 1999; Stefan and Preud'homme, 1993). Previous studies suggested a lag of 0–20 days based on daily simulations of stream temperature (Ficklin et al., 2012a; van Vliet et al., 2011). It's noteworthy that the time lag here has different meaning to those derived from autocorrelation analysis between the air and water temperature (Webb et al., 2003). The time lag is used here to calculate the moving average of antecedent air temperature, based on which the stream temperature prediction can be optimized according to the prescribed objective functions. The parameter λ (−) and ε (°C) are calibration coefficients to represent the overall effects of air–landscape–water heat transfer during the time of concentration for a specific subbasin. The air temperature addition coefficient ε is applied to allow water temperature pluses when $T_{air,lag}$ is below ε. In our previous study, the coefficient ε was determined to be between 0 and 4.5 °C for selected watersheds in the western United States.

In addition to the processes associated with water mixing and routing in a stream, stream-level simulation adjusts stream temperature ($T_{w,stream}$) based on heat exchange,

$$T'_{w,stream} = T_{w,stream} + K \cdot TT \cdot \left(T_{air,lag} - T_{w,eq}\right) \quad (8)$$

where T and T′ are stream temperature before and after the heat exchange adjustment, respectively, K (1/h) is a bulk coefficient of heat transferability with range of 0 to 1, TT (h) is the hydraulic retention time or water travel time through the stream segment within the subbasin. During the model simulation, a minimum water temperature of 0.1 °C is applied to all predicted T_w's in above Eqs. (6) to (8). Compared to our previous study (Ficklin et al., 2012a), the model in this study is designed to provide a more consistent simulation of stream temperature for highly-variable hydrologic conditions such as snowmelt-driven systems. The model introduce the concept of equilibrium temperature to normalize the water temperature responses to the air temperature over a year, thus to avoid seasonal calibrations as required in the previous study.

2.2.3. SWAT updating and application

SWAT version 2009 was selected as the base model for modification and integration. SWAT 2009 is the latest version at the time of this study with full documentation and support from the developers. Source code for SWAT was obtained from the official website (http://swatmodel.tamu.edu/software/swat-model/). The original SWAT was updated by incorporating the dynamic concentration of CO_2, the CO_2 effects on PET calculation, and the new model for stream temperature prediction, and compiled as a new program ("updated SWAT", thereafter).

In addition to the model parameters required by the original SWAT, more variables were needed for the updated SWAT. Projected CO_2 concentrations for each year of the 21st century were obtained from IPCC Data Distribution Center (http://www.ipcc-data.org/ddc_co2.html). Parameter values of *c* and *l* in formulating CO_2 impacts on PET were taken from the literature and summarized in Table 1. The four parameters (λ, *K*, ε, and *lag*) for stream temperature prediction were calibrated based on measured data.

Due to the introduction of additional parameters in the stream temperature prediction, the existing tools of automatic calibration designed for the original SWAT, including ArcSWAT (Winchell et al., 2011) and SWAT-CUP (Abbaspour, 2011), are not appropriate in this study. A program was developed based on the Sequential Uncertainty Fitting (SUFI) procedure (Abbaspour et al., 2004) with parallel computations to optimize input parameters for streamflow and stream temperature predictions. The SUFI procedure combines optimization with uncertainty analysis and can handle a large number of parameters. The objective function was defined to maximize the Nash–Sutcliffe efficiency (NSE) (Nash and Sutcliffe, 1976) between observations and predictions at the outlet of each selected watersheds. RMSE (root-mean-square error) and PBIAS (percent bias) were also provided as additional statistics for model performance. According to guidelines for evaluating watershed simulations, "satisfactory" simulations can be judged by statistics of NSE > 0.5 and PBIAS ± 25% for streamflow (Moriasi et al., 2007). In addition, the simulation results were considered to be "good" if NSE was larger than 0.75 (Larose et al., 2007; Van Liew and Garbrecht, 2003).

2.3. Site description and simulation design

The updated SWAT was applied to headwater drainage basins in the northern Coastal Ranges and Sierra Nevada mountain range in California (Fig. 1). As important water supplier for California, those ranges are associated with higher annual precipitation than the state average. The Coastal Ranges extend with a general northwest to southeast orientation along the California coast, and include most of the mountain ranges between the Klamath Mountains and Transverse Ranges. The Sierra Nevada runs 640 km north-to-south in California and Nevada. The western Sierra is drained by Sacramento River and San Joaquin River, two major watercourses of the California' Central Valley, and their tributaries. In addition to local water supply, the northern Coastal Ranges and Sierra Nevada also function as significant water suppliers to other parts of California. A number of rivers with year-round streamflow in the study area also support substantial habitats to several species of salmon and steelhead trout. Climate change, together with urbanization and agricultural development, are increasingly impacting the availability and sustainability of limited water resources in the ranges, resulting in population decline for various aquatic species (Feyrer et al., 2007; Moyle et al., 2011; Richter and Kolmes, 2005).

Site selection in this study was based on the considerations of [1] spatial coverage of the study area, [2] monitoring data availability of both streamflow and stream temperature, and [3] natural flow conditions with minimal effects of hydrologic modifications such as dams and diversions. Selected monitoring sites (Table 2) represented drainage areas of small rivers or headwaters which are generally enclosed a single eight-digit hydrologic unit code (HUC). All sites are actively monitoring by USGS for streamflow and stream temperature at the time of study, with some historical data missing. For each site, SWAT model was calibrated and validated by daily predictions of streamflow and stream temperature during a ten-year simulation period of the last decade (2001–2010), except for the gauge #11264500 for which the simulation period is set to 1981–1990 according to the data availability. The calibrated models were further applied to the projected climate data for 2001–2099 for evaluating the effects of climate change on SWAT predictions.

Except for watershed [9] (South Fork Tule River near Porterville, #18930006), average annual precipitation of the selected headwater drainage basins are over 1000 mm (Table 2), much higher than the statewide average of about 500 mm/year. The studied basins are generally associated with a Mediterranean climate, with rainy winter and dry summers. More than 50% of annual precipitation is contributed by the winter months conventionally defined as December to February. Some of the tested watersheds are snowmelt-driven hydrologic system, such as [1] (Trinity River at Hoopa, #11530000), [7] (Tuolumne River at Grand Canyon, #11274790), [8] (Merced River near Yosemite, #11264500), and [9] (South Fork Tule River near Porterville, #11204100). Compared to others in this study, those watersheds are associated with more snow accumulation according to the National Snow Analysis (http://www.nohrsc.noaa.gov/nsa/). Therefore, high streamflow rates for those sites are mainly observed for the snowmelt season from March through June, total flow volume in those months accounted for 60-70% of annual flow. For other basins in this study, monthly distribution of streamflow is generally correlated to precipitation, and more than 50% of annual flow is attributed to the winter seasons. The selected watersheds are mainly

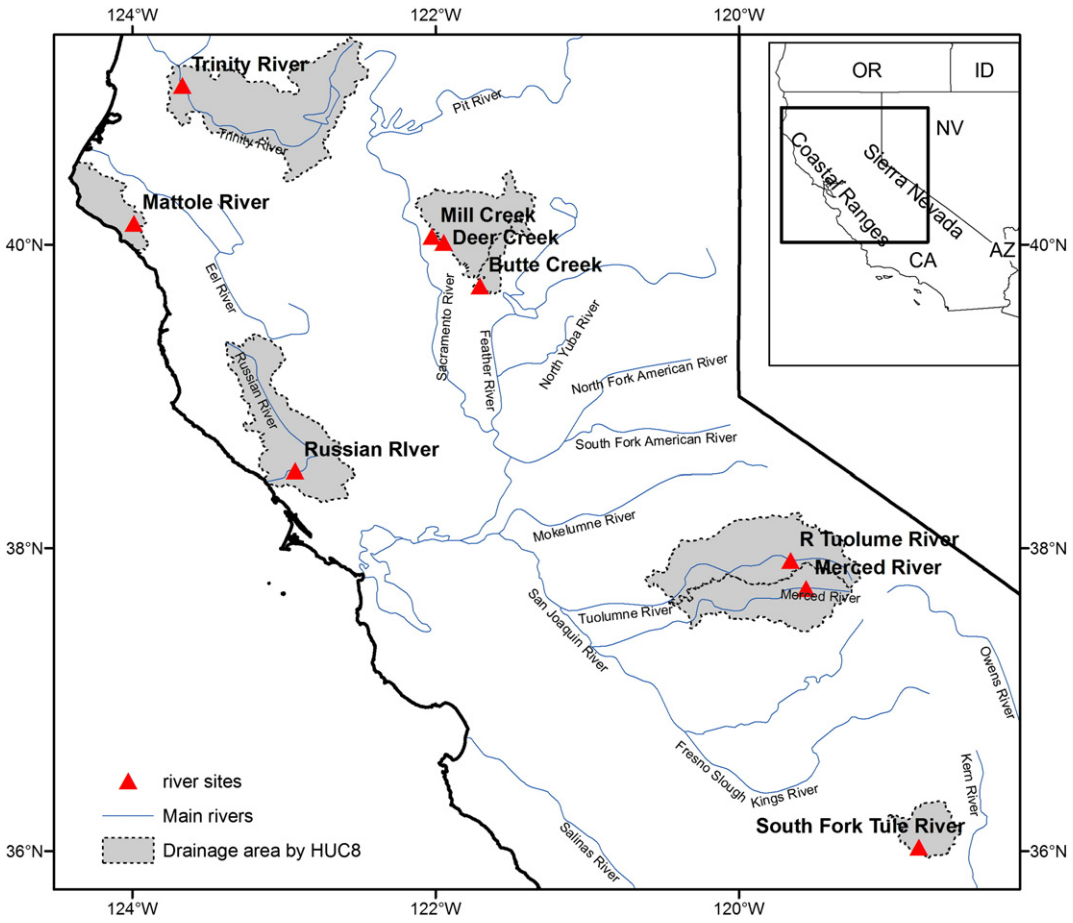

Fig. 1. Selected watersheds for model evaluation in this study, background raster for annual precipitation from high (blue) to low (red).

covered by coniferous forest, deciduous forest, and rangeland, which require plant-specific values for the stomatal conductance reduction and maximum LAI increase with elevated CO_2 concentration (Table 1).

SWAT parameters for hydrologic simulation were initialized within the ArcSWAT interface (Winchell et al., 2011). Input data for watershed morphology, including the National Elevation Dataset (NED), GIRAS land use, and National Hydrography Dataset (NHD), were obtained from the BASINS database maintained by U.S. Environmental Protection Agency (USEPA, 2007). Soil data was retrieved from Soil Survey Geographic (SSURGO) Database, and processed by the procedures presented in our previous study (Luo et al., 2012). Daily data of precipitation, maximum and minimal temperatures, and wind speed were obtained from gridded observed meteorological data (Maurer et al., 2002). The dataset is at 1/8 degree (~12 km) spatial resolution, and recently extended to include data up to year 2010 (http://www.engr.scu.edu/~emaurer/data.shtml). For the climate change study, downscaled climate projections with daily data of precipitation, maximum and minimum temperatures, and wind speed from 2001 to 2099 was taken from the Green Data Oasis (http://gdo-dcp.ucllnl.org) (Maurer et al., 2007). The data was downscaled form the native-scale outputs from climate models to a 1/8 degree grid using the well-established bias-correction and spatial disaggregation (BCSD) method (Wood et al., 2002, 2004). All available climate projections for the greenhouse gas emission scenario A2 (higher greenhouse gas emissions) and B1 (lower emissions) in the database, i.e., 36 projections for A2 and 37 for B1 with details in Supplementary Materials, were used in this study in order to capture the variations and uncertainty of climate response to future increased greenhouse gas levels. Solar radiation and relative humidity was generated by the WXGEN weather generator (Sharpley and Williams, 1990). This generator has been fully incorporated in SWAT with monthly climatic statistics from historical data over United States. These statistics were left invariant in the model simulations under climate change scenarios due to data limitation.

3. Results and discussion

3.1. Hydrological simulation

Model performance was first evaluated for streamflow prediction with measured data during 2001–2010 (except for watershed [8] with 1981–1990), with the first 5 years for model calibration and the last 5 years for validation. Input parameters to be calibrated were selected based on our previous studies (Ficklin et al., 2012b; Luo et al., 2008) and preliminary sensitivity analysis, mainly including the SCS runoff curve number (CN), snowmelt-related parameters, channel hydraulic conductivity, and parameters for groundwater recharge (see Supplementary Material for the list of parameters). Hydrologic calibration in this study was simplified by uniformly altering each input parameter for the entire drainage basin to optimize the prediction of streamflow. For example, a CN2 (CN for moisture condition II) adjustment of −10% for a specific watershed suggested that CN2 values in all upstream HRUs will be decreased by 10% from the corresponding initial values assigned by ArcSWAT. Further calibration, especially with spatially distributed parameterization, may improve the model performance, but increases the modeling complexity and goes beyond our study scope.

The performance of the calibrated models in simulating daily streamflow is summarized in Table 3, and the modeling results were plotted with observations in Supplementary Materials. For

Table 2
Site descriptions for (a) the USGS gauges selected in this study and (b) their drainage areas.

(a) information of river sites

ID	USGS site # and name	Latitude	Longitude	Elevation (m)	Average streamflow (cms)	Average stream temperature (°C)
[1]	11530000 (Trinity River at Hoopa, CA)	41.05	−123.67	84	119.6	13.3
[2]	11468900 (Mattole River near Ettersburg, CA)	40.14	−123.99	176	8.0	12.5
[3]	11381500 (Mill Creek near Los Molinos, CA)	40.05	−122.02	117	7.8	12.9
[4]	11383500 (Deer Creek near Vina, CA)	40.01	−121.95	146	6.6	13.7
[5]	11390000 (Butte Creek near Chico, CA)	39.72	−121.71	45	9.4	12.6
[6]	11467000 (Russian River near Guerneville, CA)	38.51	−122.93	6	47.7	16.0
[7]	11274790 (Tuolumne River at Grand Canyon above Hetch Hetchy)	37.92	−119.66	1167	18.3	9.0
[8]	11264500 (Merced River near Yosemite, CA)	37.73	−119.56	1228	11.6	7.5
[9]	11204100 (South Fork Tule River near Porterville, CA)	36.02	−118.81	296	1.2	15.0

(b) information of the drainage area

ID	USGS site #	Enclosing HUC	Drainage area (km^2)	Average elevation (m)	Precipitation (mm/year)	Average air temperature (°C)	
						January	July
[1]	11530000	18010211	7304	991	1051	0.5	19.4
[2]	11468900	18010107	149	445	1895	7.9	15.5
[3]	11381500	18020119	335	798	1301	1.0	20.0
[4]	11383500	18020119	532	1146	1301	3.1	22.3
[5]	11390000	18020120	376	1073	1467	5.4	24.3
[6]	11467000	18010110	3425	267	1094	7.4	21.5
[7]	11274790	18040009	771	2526	1126	−6.4	15.2
[8]	11264500	18040008	463	2582	1189	−5.1	15.8
[9]	11204100	18030006	245	1232	538	4.8	24.3

Notes: [1] the identification number (ID) is used as index to the river site and the drainage watershed of the site; [2] the enclosing HUC is the 8-digit HUC where the majority of drainage area of the corresponding site is located. The sites themselves may be in a downstream hydrologic unit. For example, the sites #11381500 and 11383500 are in the HUC of 18020103, but 98% of their drainage areas are in the HUC of 18020119. [3] Averages of climate variable and river measurements are based on data from 2001 to 2010, except for watershed [8] (Merced River near Yosemite, #11264500) for which simulations are based on data during 1981–1990 due to its data limitation in stream temperature measurements. cms = cubic meter per second.

each site, the values of goodness-of-fit statistics (NSE, RMSE, and PBIAS) were similar for the calibration and validation periods. Therefore, the statistics are only reported for the whole 10-year simulation period. With appropriate calibrations, SWAT generated satisfactory (NSE > 0.50) results in comparison with the observed data of daily streamflow at the outlets of selected watersheds. The average NSE of the studied watershed was 0.68, ranging from 0.51 to 0.81. In some watersheds, SWAT failed to capture the flood events with extremely high flow rate during winter season. At gauge #11530000, for example, SWAT underestimated flood events with flow rate > 1500 cms (or the 99.992th percentile of daily measurements during the 10-year period). This may be related to the homogeneous assumption of SWAT, e.g., basin-wide average parameters for snowmelt simulation and one set of parameters for all channels in each subbasin. In addition, SWAT is not designed to simulate detailed, single-event flood routing (Neitsch et al., 2011).

For comparison with other studies of streamflow prediction in California, monthly statistics between observed and predicted streamflow are also reported in this study (Table 3). According to the reported NSE values, SWAT simulations in this study generate comparable modeling performance to our previous modeling studies in the foothills of Costal Range (Luo et al., 2008) and in the Sierra Nevada (Ficklin et al., 2012b). In addition, this study reported monthly RMSE normalized by average observations of 27%–57%, comparable to the results of 38%–65% reported by Young et al. (2009) based on hydrologic simulations with WEAP (Water Evaluation and Planning System) for the Sierra Nevada. In summary, the calibrated models were considered suitable in establishing a reliable hydrological framework for further studies of stream temperature and climate change.

Table 3
Statistics comparing observed and predicted daily streamflow at the selected sites in this study.

ID	USGS site #	Daily simulation results			Monthly averages		
		NSE	RMSE (cms)	PBIAS	NSE	RMSE (cms)	PBIAS
[1]	11530000	0.74	83.56	0.11	0.87	45.55	0.11
[2]	11468900	0.67	11.38	−0.11	0.88	4.60	−0.12
[3]	11381500	0.52	6.57	0.06	0.85	2.33	0.06
[4]	11383500	0.70	6.81	0.22	0.83	3.40	0.22
[5]	11390000	0.73	7.92	0.14	0.80	4.60	0.14
[6]	11467000	0.73	70.08	0.15	0.86	32.24	0.15
[7]	11274790	0.51	5.29	−0.24	0.70	3.82	−0.24
[8]	11264500	0.81	7.35	−0.11	0.90	4.75	−0.10
[9]	11204100	0.68	0.78	−0.17	0.77	0.30	−0.17

Notes: The site ID refers to that in Table 2. The simulation period is 2001–2010 except for #11264500, for which the 10-year period of 1981–1990 was used according to the data availability of stream temperature. cms = cubic meter per second.

3.2. Stream temperature simulation

Based on the calibrated model for streamflow, the SWAT was utilized to simulate stream temperature at daily time step for the same 10-year period. Two sets of simulations were conducted based on [1] the original SWAT with linear model for stream temperature simulation, and [2] the updated SWAT with the new stream temperature model. The linear model is only dependent on the average air temperature, Eq. (5), thus no calibration is required. For the newly developed model, similar to model evaluation for streamflow simulation, measured data of stream temperature for the first 5 years were used for model calibration, while the last 5 years were used for validation. For each monitoring site of stream temperature, the update SWAT was calibrated with four parameters (λ, K, ε, and lag) by comparing the observed and predicted daily stream temperature. Parameter alteration was conducted on drainage area basis, i.e., the numerical value of a specific parameter would change simultaneously for all upstream subbasins of a monitoring site. Therefore, the calibrated parameters actually represented average thermal properties of the entire drainage area of the site. This approach is justified by the fact that stream temperature at a downstream is location potentially affected by heat sources and transfers of upstream landscape and waterways.

Table 4 compares the model performance of stream temperature prediction by the linear model in the original SWAT and the new model of stream temperature prediction in updated SWAT. For all watersheds

Table 4
Model performance and calibrated parameters for daily stream temperature prediction.

(a) Model performance

		The original SWAT			The updated SWAT		
ID	USGS site #	NSE	RMSE (°C)	PBIAS	NSE	RMSE (°C)	PBIAS
[1]	11530000	0.83	2.25	0.09	0.91	1.66	0.01
[2]	11468900	0.62	3.08	0.01	0.74	2.52	−0.01
[3]	11381500	0.52	3.89	0.26	0.88	1.91	0.002
[4]	11383500	0.53	4.37	0.28	0.82	2.69	0.05
[5]	11390000	0.80	2.47	−0.12	0.84	2.17	0.02
[6]	11467000	0.80	2.10	0.07	0.83	1.93	0.03
[7]	11274790	0.78	2.87	0.17	0.89	2.03	−0.002
[8]	11264500	0.64	2.93	−0.30	0.85	1.90	0.02
[9]	11204100	0.83	2.66	−0.13	0.90	2.00	0.002

(b) Calibrated parameters in the updated SWAT for stream temperature prediction

ID	USGS site #	λ	K (1/h)	ε (°C)	lag (day)
[1]	11530000	1.11	0.06	5.84	9
[2]	11468900	1.32	0.04	5.33	7
[3]	11381500	0.97	0.07	5.98	2
[4]	11383500	1.25	0.05	7.09	2
[5]	11390000	0.78	0.13	2.69	8
[6]	11467000	1.04	0.04	5.38	3
[7]	11274790	1.29	0.39	5.65	8
[8]	11264500	1.07	0.01	5.70	5
[9]	11204100	1.00	0.27	5.04	7

Note: The site ID refers to that in Table 2.

in this study, the updated SWAT improved stream temperature simulations compared to the original one. Average model performance statistics of NSE and RMSE were 0.85 and 2.09 °C, respectively, for the updated SWAT; and NSE of 0.70 and RMSE of 2.96 °C for the original SWAT. The averages of the absolute PBIAS were 1.5% and 15.9% for the updated and original SWAT, respectively. While there are no strict criteria of acceptable model performance in stream temperature prediction, statistics in Table 4 were compared to those reported in previous studies. For example, Mohseni et al. (1998) reported average NSE of 0.93 and average RMSE of 1.64 °C (weekly simulation) in 584 USGS gauges, van Vliet et al. (2011) reported average NSE of 0.85 and average RMSE of 2.26 °C (daily simulation) for worldwide major rivers, and Ficklin et al. (2012a) reported average NSE of 0.82 (daily simulation) for 7 watersheds in western United States.

Further investigation indicated that the original SWAT generated relatively poor predictions for winter and summer seasons. This is related to the fact that stream temperature responses to air temperature deviate from linearity for high or low air temperatures (Mohseni and Stefan, 1999; Mohseni et al., 1998). The NSE by the original SWAT for summer season of June to August averaged at −1.42, while the updated SWAT had better predictions during the same period with average NSE of 0.56. Reliable prediction of summer stream temperature is required by risk assessment and management planning for healthy aquatic habitats.

3.3. Effects of climate change

3.3.1. Climate changes characterized by the selected projections

Table 5 summarizes the changes of precipitation, air temperature, and wind speed as annual average between two 10-year periods of 2089–2099 and 2001–2010 based on the selected GCM projections for the grid nodes close to the USGS gauges (Table 2). In this study, changes of hydrologic components such as precipitation, streamflow, and ET were presented in a relative format (%). Absolute changes were reported for air temperature (°C) and wind speed (m/s).

Decreases in precipitation were observed at most of the watershed in this study, especially under the A2 scenarios, but none of them were statistically significant. Relative to air temperature and wind speed, the changes of precipitation were associated with much higher variability to projections and to the geographic locations (Fig. 2). The great uncertainty in the GCM-predicted precipitation should be considered when presenting climate change and its effects on the predictions of hydrologic and environmental components. Significant increases of air temperature were observed for all studied watersheds, with median increases of 3.0–3.8 °C with the A2 scenarios, and about 1.5 °C with the B1 scenarios. Changes of air temperature in the B1 scenarios were associated with higher uncertainty relative to the A2 ones, suggested by the coefficient of variations averaged 0.4 and 0.2, for the B1 and A2 scenarios, respectively. Similarly, GCM data indicated that wind speed consistently increased by 0.2 m/s with the A2 scenarios and 0.1 m/s with the B1 scenarios for all simulated watersheds, generally proportional to the magnitudes of air temperature increases.

Further analysis on monthly data concluded uneven changes of precipitation over a year (Fig. 3 with the watershed of Trinity River at Hoopa, USGS#11530000 and watershed of Tuolumne River at Grand Canyon, #11274790 as examples). Generally significant increases of precipitation are observed during winter rainfall seasons, while for summer months decreases in precipitation are frequently predicted. In addition to the general decreasing trend of annual precipitation with high uncertainty observed for most of the watersheds (Table 5), GCM data characterizes the future climate of California with wetter winters and drier summers. Similarly, temperature increase is greater in summer than in winter, especially for the A2 scenarios, which would have significant effects on plant growth, water quality, and ecosystem health. Those findings are consistent to the results in other studies (Cayan et al., 2009; Pan et al., 2011; Pierce et al., 2012). No substantial seasonal pattern was detected for the changes of wind speed.

3.3.2. Sensitivity to the changes on individual climate variables

Before the investigation of the integrated effects of climate change on hydrologic and water quality predictions, sensitivity analysis to the individual climate variables (CO_2 concentration, air temperature, and precipitation) were conducted by changing one-factor-at-a-time (OAT). CO_2 concentration, with reference value of 330 ppm, was set to 846 and 544 ppm for the A2 and B1 scenarios (IPCC, 2000). Changes on the air temperature and wind speed were selected to represent the expected values in the study area (Table 5). In summary, air temperature was increased by 3.5 (A2) and 1.5 °C (B1), while wind speed was increased by 0.2 (A2) and 0.1 (B1) m/s. Since no statistically significant trend was detected for precipitation, its relative change was assigned with arbitrary values of ±10%. The adjustments on precipitation, air temperature, and wind speed were uniformly applied to all months during the simulation period.

A sensitivity index (S) was defined to compare the results of OAT analysis (Lenhart et al., 2002; Luo et al., 2008),

$$S = \frac{\Delta P}{\Delta I}\frac{I_0}{P_0} \tag{9}$$

where P is the dependent variable in the sensitivity analysis, such as streamflow, ET, and stream temperature in this study, and I is the climatic variables including CO_2 concentration, precipitation, air temperature, and wind speed. The sensitivity index provided a transfer function to propagate the relative error of the input variables into the relative error of the prediction. Results indicated that variation of ET was mainly determined by air temperature and moderately contributed by precipitation and wind speed (Table 6). As expected, the prediction of streamflow was mainly sensitive to precipitation. The sensitivity index of about 1.3 suggested that 10% increase or decrease of precipitation would result in 13% change in streamflow on an annual basis. For stream temperature, air temperature was the most sensitive parameter.

Changes in precipitation proportionally affect annual streamflow in all watersheds, mainly resulting from the change of surface runoff amount especially during winter rain season (Table 7). About ±1% changes in ET flux were predicted with precipitation changes

Table 5
Annual average of climatic variables during 2090–2099 relative to those during 2001–2010 for the selected GCM projections, expressed as median changes and their IQRs (in parentheses).

ID	USGS site #	Δ Precipitation (%)		Δ Average air temperature (°C)		Δ Wind speed (m/s)	
		A2	B1	A2	B1	A2	B1
[1]	11530000	1.2 (25.2)	−1.0 (17.2)	3.1 (1.0)	1.4 (0.8)	0.2 (0.1)	0.1 (0.1)
[2]	11468900	0.6 (21.7)	2.8 (19.0)	3.0 (1.0)	1.4 (0.8)	0.2 (0.1)	0.1 (0.1)
[3]	11381500	−0.5 (24.5)	2.2 (20.1)	3.6 (1.2)	1.5 (0.9)	0.2 (0.1)	0.1 (0.1)
[4]	11383500	−0.5 (24.5)	2.2 (20.1)	3.6 (1.2)	1.5 (0.9)	0.2 (0.1)	0.1 (0.1)
[5]	11390000	−1.6 (24.1)	0.8 (21.6)	3.6 (1.3)	1.6 (0.9)	0.2 (0.1)	0.1 (0.1)
[6]	11467000	−2.6 (26.4)	1.2 (22.3)	3.1 (1.0)	1.4 (0.9)	0.2 (0.1)	0.1 (<0.1)
[7]	11274790	−9.4 (29.6)	−1.5 (27.4)	3.8 (1.6)	1.6 (0.9)	0.2 (0.1)	0.1 (0.1)
[8]	11264500	−9.7 (29.5)	−2.0 (25.8)	3.8 (1.5)	1.6 (0.9)	0.2 (0.1)	0.1 (0.1)
[9]	11204100	−14.1 (33.2)	−5.7 (24.4)	3.8 (1.5)	1.6 (0.9)	0.2 (0.1)	0.1 (0.1)

Note: The site ID refers to that in Table 2. According to the Wilcoxon test results, all the changes on precipitation are not significant ($p>0.05$), and all the changes on average air temperature and wind speed are significant ($p<0.001$).

of ±10%, which could be related to the corresponding changes in soil water content. Precipitation change also had detectable effects on stream temperature especially during summer months, although the annual average sensitivity was very small. Stream temperature was impacted by precipitation through its influence on streamflow rate: increased streamflow and decreased hydraulic retention time would reduce stream temperature according to Eq. (8). Changes in stream temperature were significantly correlated to those of average air temperature. The ratio between changes in air temperature and stream temperature was about 0.8 for both scenarios A2 and B1, suggesting the air temperature increase of 1 °C would result in an increase of 0.8 °C of stream temperature as annual average. As expected, a higher air temperature increased ET and decreases stream temperature, but did not have significant effects on annual streamflow.

The median reduction of ET was 3.11% over the selected watersheds with the increase of CO_2 concentration under the A2 scenario (846 ppm), and 1.27% under the B1 scenario (544 ppm). The magnitude of relative ET reduction was mainly related to the landuse types in a watershed. For all tested watersheds, the average reductions of ET were 10.6% for agricultural land, 5.7% for deciduous forest, 4.2% for rangeland, and 2.2% for coniferous forest, by solely doubling CO_2 concentration. The resultant reductions were significantly correlated to the percent change of stomata conductance (c value, $r=-0.99$, $p=0.01$) in response to the doubling of CO_2 concentration (Table 1). By decreasing ET, the elevated CO_2 concentration has positive effects on streamflow. However, the sensitivity index of streamflow to ET, $(\Delta Q/Q)/(\Delta ET/ET)$ varied with watersheds. Further data analysis indicated moderate association between the sensitivity and the aridity index (PET/P, where P is annual average precipitation) over the tested watersheds ($r=-0.70$, $p=0.03$). This funding suggested that streamflow in arid area might be more sensitive to the change of CO_2 concentration.

To demonstrate the SWAT modifications in the study, model simulations were conducted with and without the CO_2 adjustments on the calculations of stomatal conductance and leaf area index. Comparison here was based on the modeling results at the watershed of Trinity River at Hoopa (USGS#11530000), which is mainly covered by FRSE (88%). In the original SWAT with $c=0.4$ for all vegetation and no consideration of CO_2-dependence of LAI_{mx} ($l=0$), the predicted ET reduction was 18% and 6% under the B2 and A1 scenarios, repetitively. The effects of CO_2 are significantly alleviated by introducing the less reduction of stomatal conductance and greater LAI_{mx} under elevated CO_2 concentration. When adjusting c to small values such as 0.08 for FRSE, predicted ET reduction was decreased to 2% under the A2 scenario, and 1%

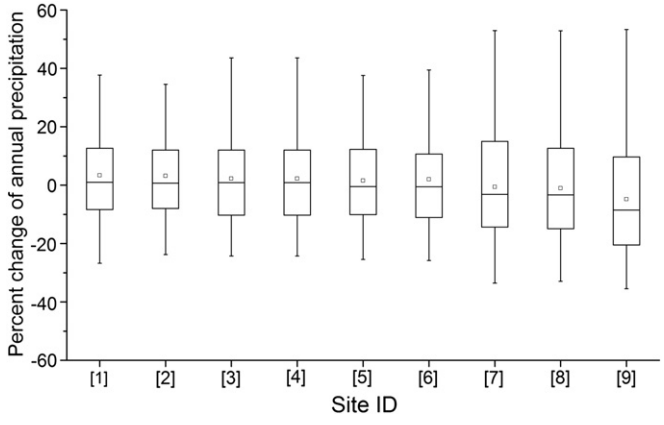

Fig. 2. Percent change of annual precipitation of 2090–2099 relative to that of 2001–2010 under the A2 and B1 projections. Squares indicate mean values. Outliers are not shown. Site ID refers to that in Table 2.

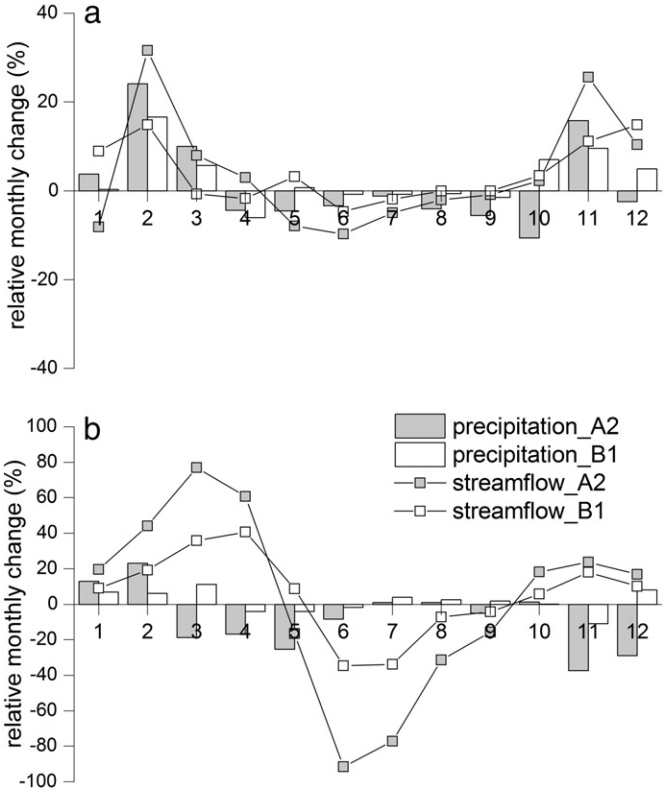

Fig. 3. Monthly changes (%) of projected precipitation and predicted streamflow normalized by the annual averages for each month, 2089–2099 vs. 2001–2010 for (a) the watersheds [1] and (b) [7] (Table 2).

Table 6
Sensitivity index (S) of streamflow, ET, and strea, temperature to climatic variables based on sensitivity analysis by changing one factor-at-a-time (OAT), presented as median changes and IQR (in parentheses) over the selected watersheds.

OAT scenarios	ET	Streamflow	Stream temperature
CO_2_A2	−0.02 (0.02) L	0.005 (0.003) N	0 (0) L
CO_2_B1	−0.02 (0.02) L	0.005 (0.002) N	0 (0) L
pcp + 10%	0.13 (0.11) M	1.30 (0.08) VH	−0.02 (0.03) N
pcp-10%	0.14 (0.12) M	1.28 (0.10) VH	−0.02 (0.06) N
+3.5 °C	0.33 (0.24) H	−0.07 (0.12) M	0.71 (0.29) H
+1.5 °C	0.34 (0.22) H	−0.07 (0.15) M	0.64 (0.26) H
+0.2 m/s	0.09 (0.20) M	−0.04 (0.09) N	0 (0) L
+0.1 m/s	0.07 (0.21) M	−0.04 (0.09) N	0 (0) L

Notes: VH: very high sensitivity (|S|≥1); H: high (|S|≥0.2); M: moderate (|S|≥0.05), and L: low (|S|<0.05) (Lenhart et al., 2002).

under the B1 scenario. Accordingly, the expected increase of streamflow would be also alleviated, from 4.9% to 0.6% (A2), and 1.5% to 0.2% (B1).

3.3.3. Integrated effects

For each of the tested watersheds, the calibrated SWAT for streamflow and stream temperature was applied to the climatic projections from the 73 GCMs for 2001–2099. Daily predictions during two 10-year periods of 2001–2010 and 2090–2099 were extracted from the model simulations. Similar to the quantification of climate change, the responses of predicted streamflow and stream temperature to climate change were defined as their changes between the two periods, as 10-year annual averages or long-term monthly averages. Compared to the OAT-based sensitivity analysis, model applications with GCM data reflected the integrated effects of climate variables on hydrologic and water quality simulations. In addition, the sensitivity analysis assumed uniform changes of climate variables in a year, while by using GCM data the projected seasonal dynamics of climate change can be incorporated in the SWAT simulation. Predicted increases of annual average stream temperature were 2.1–3.5 °C under the A2 scenario and 1.0–1.6 °C under B1 scenario, generally proportional to the projected increases of average air temperature (Table 8). Similarly, strong linearity between climate change and modeled changes on hydrologic components was detected for all watersheds. Taking the watershed [1] as an example, changes in annual average streamflow predicted by SWAT was significantly correlated to the precipitation changes, $r = 0.971$ ($p < 0.001$) for the A2 projections and $r = 0.975$ ($p < 0.001$) for the B1 projections. Positive interceptions (about +4% for the watershed [1]) were observed in the linear regression between precipitation change and streamflow change, suggesting an increasing trend of annual average streamflow even with invariant amount of annual precipitation. This is associated with positive effects of elevated air temperature and CO_2 concentration on streamflow in the study area. It also explained the general increases of predicted streamflow (Table 8) during 2090–2099 in comparison to current condition (2001–2010), although not all of the increases were statistically significant.

Table 7
Results of climate sensitivity analysis by changing one factor-at-a-time (OAT), presented as median changes and IQR (in parentheses) over the selected watersheds.

OAT scenarios	Δ ET (%)	Δ Streamflow (%)	Δ Stream temperature (°C)
CO_2_A2	−3.11 (3.58) **	0.80 (0.51) **	0.00 (0.00) NS
CO_2_B1	−1.27 (1.39) **	0.30 (0.14) **	0.00 (0.00) NS
pcp + 10%	1.29 (1.15) **	13.05 (0.84) **	−0.03 (0.04) *
pcp-10%	−1.44 (1.18) **	−12.84 (1.05) **	0.03 (0.07) *
+3.5 °C	8.81 (2.56) **	−2.26 (2.91) **	2.88 (0.53) **
+1.5 °C	3.75 (2.60) **	−1.06 (1.34) **	1.20 (0.20) **
+0.2 m/s	0.62 (1.49) *	−0.32 (0.89) **	0.00 (0.00) NS
+0.1 m/s	0.26 (0.77) *	−0.16 (0.46) **	0.00 (0.00) NS

Note: Statistical significances based on the Wilcoxon test, where *: $p<0.05$, **: $p<0.01$, ***: $p<0.001$, NS: not significant ($p>0.05$).

Table 8
Changes of predicted annual averages of streamflow and stream temperature under the selected GCM projections, presented as median and IQR (in parentheses) over the selected climate projections.

		Δ Streamflow (%)		Δ Stream temperature (°C)	
ID	USGS site #	A2	B1	A2	B1
[1]	11530000	5.9 (37.4) *	3.2 (26.0) *	2.6 (0.9) ***	1.2 (0.7) ***
[2]	11468900	4.8 (36.0) NS	1.8 (23.1) NS	3.5 (1.1) ***	1.6 (1.0) ***
[3]	11381500	0.1 (36.7) NS	3.5 (27.0) NS	2.2 (0.8) ***	1.0 (0.6) ***
[4]	11383500	0.2 (35.4) NS	4.7 (27.1) NS	2.7 (0.9) ***	1.2 (0.7) ***
[5]	11390000	1.0 (37.0) NS	7.0 (32.6) *	2.2 (0.8) ***	1.0 (0.6) ***
[6]	11467000	4.1 (48.3) NS	8.2 (39.2) *	2.5 (0.7) ***	1.1 (0.7) ***
[7]	11274790	−2.3 (38.9) NS	8.4 (33.8) **	2.7 (1.2) ***	1.2 (0.7) ***
[8]	11264500	−1.4 (37.0) NS	4.5 (26.0) **	2.1 (0.8) ***	1.0 (0.5) ***
[9]	11204100	7.4 (52.6) **	17.7 (61.3) ***	2.7 (1.1) ***	1.2 (0.8) ***

Notes: The ID refers to that in Table 2. Statistical significances based on the Wilcoxon test, where *: $p<0.05$, **: $p<0.01$, ***: $p<0.001$, NS: not significant ($p>0.05$).

As mentioned before, GCM data suggests increased precipitation during cold seasons and decreases in warm seasons at the end of the 21st century (Fig. 3), although annual total precipitation would not significantly change (Table 5). Therefore, increased streamflow during winter months and decreased streamflow during summertime were predicted for all watersheds (watersheds [1] and [7] are demonstrated in Fig. 3, other watershed in Supplementary Materials). The overall changes on annual streamflow were mainly determined by the seasonal distribution of precipitation and the weather pattern of the watershed. Generally, significant reductions of annual streamflow were mainly associated with the snowmelt-driven watersheds and with the B1 scenarios. For watersheds significantly affected by snowmelt, a decreased streamflow as annual average under climate change scenarios might be predicted since majority of flow volume in those watersheds are contributed by spring and summer months. For watersheds affected by snowmelt, in addition, the seasonality of precipitation change was significantly magnified in the resultant seasonality of streamflow. For example, in watershed [7] the median monthly changes of precipitation ranged from −37% to +23% for the A2 scenarios, while the predicted changes in streamflow were −92% to +77% (Fig. 3). This might be explained by the effects of air temperature on snowmelt-driven hydrologic system: increased air temperature during winter seasons results in more precipitation in the form of rainfall rather than snowfall, and significantly shifted the streamflow peaks from snowmelt season to early months compared to the baseline scenarios.

Relative to the baseline scenario, the annual average of predicted stream temperature (Table 8) increased by 2.1–3.5 °C (the A2 scenarios) and 1.0–1.6 °C (the B1 scenarios), consistent to the projected increases of air temperature (Table 5). Monthly pattern of stream temperature changes were similar in the tested watersheds, with higher increase of stream temperature during summers compared to that in wintertime (Fig. 4). Generally, stream temperature in summers was more sensitive to air temperature change. At the site [1] (Trinity River at Hoopa) under the A2 scenarios (Fig. 4), for example, stream temperature during winters (December to February) increased from 7.6 (the baseline scenario) to 8.9 °C (median of predictions), in response to the air temperature change from 5.0 to 7.7 °C, suggesting a relative sensitivity of 0.3 compare to that of 0.9 for summer months (June to September). This could be related to the injection of cold snowmelt water which would alleviate the increase of stream temperature during winters, and to the significant streamflow decreases detected during summers in the study area (Fig. 3). During summer months (June to August), median increases of predicted stream temperature of 2090–2099 relative to that of 2001–2010 were 2.7–6.1 °C under the A2 scenarios, and 1.2–2.6 °C under the B1 scenarios over the study area. A simple risk assessment on aquatic habitats was conducted by determining the probability of daily stream temperature higher than 20 °C, the maximum value of stream temperature thresholds for Pacific migratory salmonid species over various life stages (USEPA, 2003). Over

the tested watersheds, the median probability of exceedance was increased from 15% under the baseline condition to 31% (for the A2 scenarios) or 23% (B1), suggesting an 8–16% (or about 30–60 days per year) increase of undesirable condition for salmon and trout in the river segment at the watershed outlet (Table 9).

3.3.4. Summary and conclusion

In order to characterize the climate change effects on hydrology and water quality at watershed scales, CO_2 dependence of potential evapotranspiration and stream temperature prediction were incorporated in watershed modeling approach. While the incorporation and evaluation were only demonstrated in SWAT, the approach developed in this study could be adapted for other watershed models. The updated SWAT was applied to the field conditions of 9 headwater drainage basins in the Coastal Ranges and Sierra Nevada of California. After calibrations for streamflow and stream temperature, the model was used to simulate the effects of climate change on hydrologic components based on 73 climate projections with either A2 or B1 emission scenarios for the 21th century. Simulation results were presented as changes between the two 10-year periods of 2001–2010 and 2090–2099. This is one of the first modeling efforts in evaluating the ensemble of projected climate changes in terms of their significances for both water supply (streamflow in this study) and ecosystem stressors (stream temperature as an example) within a risk assessment framework.

With appropriate calibration in this study, SWAT generated satisfactory predictions of daily streamflow during a 10-year period, indicated by resultant NSE of 0.51 to 0.81 and PBIAS of −0.17 to 0.22 for the selected watersheds. For stream temperature simulation, the model well captured the spatial and temporal viability of daily stream temperature over the study area, with NSE of 0.74 to 0.91 and PBIAS of −0.01 to 0.05. Modeling performance for stream temperature prediction was significantly improved in comparison with the linear function in the original SWAT (NSE of 0.52–0.83 and PBIAS of −0.30 to 0.28).

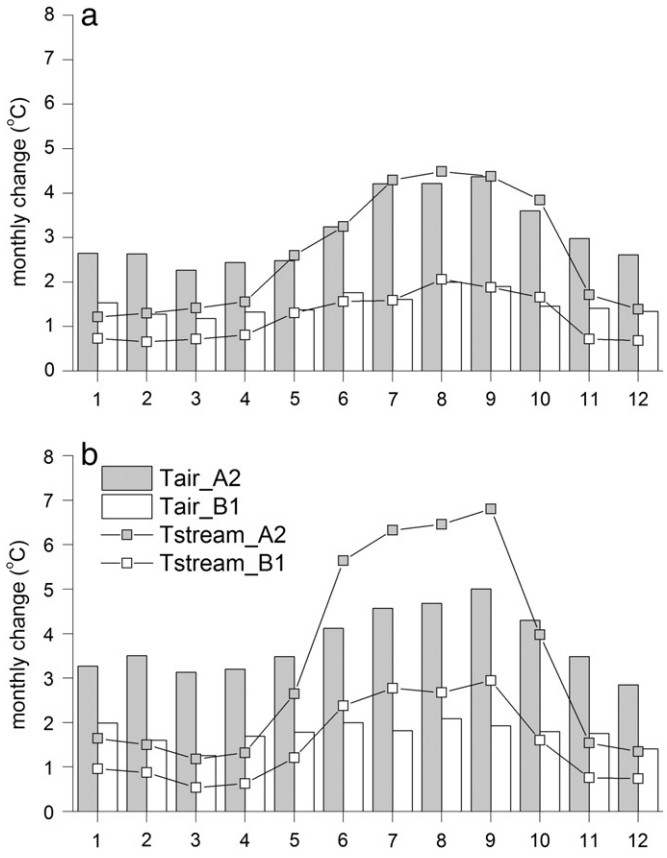

Fig. 4. Monthly changes (°C) of projected air temperature (Tair) and predicted stream temperature (Tstream) for each month, 2089–2099 vs. 2001–2010 for (a) the watersheds [1] and (b) [7] (Table 2).

Table 9
Probability of daily stream temperature exceeding 20 °C under the baseline simulation and climate projections.

ID	USGS site #	Baseline	A2	B1
[1]	11530000	0.15	0.31	0.23
[2]	11468900	0.04	0.18	0.09
[3]	11381500	0.17	0.32	0.24
[4]	11383500	0.20	0.35	0.27
[5]	11390000	0.15	0.30	0.23
[6]	11467000	0.28	0.43	0.35
[7]	11274790	0.04	0.26	0.13
[8]	11264500	0.00	0.05	0.00
[9]	11204100	0.29	0.40	0.34

Notes: The ID refers to that in Table 2. For the predictions under climate change scenarios, the median probabilities over the projections are reported.

Effects of CO_2 concentration on actual ET level were dependent on the landuse types. By solely doubling CO_2 concentration in the study area, the average reductions of ET were 10.6% for agricultural land, 5.7% for deciduous forest, 4.2% for rangeland, and 2.2% for coniferous forest. By decreasing ET, the elevated CO_2 concentration has positive effects on streamflow. Further data analysis indicated that streamflow in watersheds with higher aridity index might be more sensitive to the change in CO_2 concentration. GCM data suggests significant increases of air temperature in all tested watersheds, with median increases of 3.0–3.8 °C for the A2 scenarios, and about 1.5 °C for the B1 scenarios. Predicted increases in annual average stream temperature (2.1–3.5 °C for the A2 scenario and 1.0–1.6 °C for the B1 scenario) were general proportional to the projected increases in air temperature. Although no temporal trend was confirmed for annual precipitation in California, increases of precipitation during winter months and decreases in summers were generally observed from climatic projections. Undesirable conditions for aquatic ecosystem health were detected by data analysis on GCM projections and hydrologic simulations under climate change scenarios. First, higher air temperature increase was observed during summers than winters. In addition, streamflow decrease in summers was predicted for all watersheds in this study (caused by the decrease in precipitation and the shifting in snowmelt peaks), which further increased stream temperature during those months. Consequently, the median probability of daily stream temperature exceeding 20 °C was increased from 15% under the current condition to 31% (for the A2 scenarios) or 23% (B1) predicted at the end of the 21st century over the study area.

Appendix A. Supplementary data

Supplementary data to this article can be found online at http://dx.doi.org/10.1016/j.scitotenv.2013.02.004.

References

Abbaspour KC. SWAT-CUP4: SWAT calibration and uncertainty programs—a user manual. Dübendorf, Switzerland: Swiss Federal Institute of Aquatic Science and Technology; 2011 [http://www.eawag.ch/forschung/siam/software/swat/index].

Abbaspour KC, Johnson CA, van Genuchten MT. Estimating uncertain flow and transport parameters using a sequential uncertainty fitting procedure. Vadose Zone J 2004;3(4):1340–52.

Boyer C, Chaumont D, Chartier I, Roy AG. Impact of climate change on the hydrology of St. Lawrence tributaries. J Hydrol 2010;384(1–2):65–83.

Candela L, Tamoh K, Olivares G, Gomez M. Modelling impacts of climate change on water resources in ungauged and data-scarce watersheds, Application to the Siurana catchment (NE Spain). Sci Total Environ 2012;440:253–60.

Cayan D, Tyree M, Dettinger M, Hidalgo H, Das T, Maurer E, et al. Climate change scenarios and sea level rise estimates from the California 2009 Climate change scenarios assessment, CEC-500-2009-014-F. Sacramento, CA: California Energy Commission; 2009.

Cohn T. Recent advances in statistical methods for the estimation of sediment and nutrient transport in rivers. Contributions in hydrology. United States National Report to the IUGG; 1995. p. 1117–24.
Dowling DC, Wiley MJ. The effects of dissolved oxygen, temperature, and low stream flow on fishes: a literature review. Illinois Natural History Survey, Aquatic Biology Technical Report 1986; 1986. [2, Springfield, IL].
Ducharne A. Importance of stream temperature to climate change impact on water quality. Hydrol Earth Syst Sci 2008;12(3):797–810.
Easterling WE, Rosenberg NJ, McKenney MS, Jones CA, Dyke PT, Williams JR. Preparing the erosion productivity impact calculator (epic) model to simulate crop response to climate change and the direct effects of CO2. Agr Forest Meteorol 1992;59(1–2): 17–34.
Eckhardt K, Ulbrich U. Potential impacts of climate change on groundwater recharge and streamflow in a central European low mountain range. J Hydrol 2003;284(1–4): 244–52.
Edinger JE, Duttweiler DW, Geyer JC. The response of water temperatures to meteorological conditions. Water Resour Res 1968;4(5):1137–43.
Feyrer F, Nobriga ML, Sommer TR. Multidecadal trends for three declining fish species: habitat patterns and mechanisms in the San Francisco Estuary, California, USA. Can J Fish Aquat Sci 2007;64(4):723–34.
Ficklin DL, Luo Y, Stewart IT, Maurer EP. Development and application of a hydroclimatological stream temperature model within SWAT. Water Resour Res 2012a;48:W01511.
Ficklin DL, Stewart IT, Maurer EP. Projections of 21st century Sierra Nevada local hydrologic flow components using an ensemble of General Circulation Models. J Am Water Resour Assoc 2012b. http://dx.doi.org/10.1111/j.1752-1688.2012.00675.x.
Field CB, Jackson RB, Mooney HA. Stomatal responses to increased CO2: implications from the plant to the global scale. Plant Cell Environ 1995;18:1214–25.
Göncü S, Albek E. Modeling climate change effects on streams and reservoirs with HSPF. Water Resour Manag 2010;24(4):707–26.
Harvey BC, Nakamoto RJ, White JL. Reduced streamflow lowers dry-season growth of rainbow trout in a small stream. Trans Am Fish Soc 2006;135:998-1005.
IPCC. Special Report on Emission Scenarios (SRES), Intergovernmental Panel on Climate Change. Cambridge, UK: Cambridge University Press; 2000.
Isaak DJ, Luce CH, Rieman BE, Nagel DE, Peterson EE, Horan DL, et al. Effects of climate change and wildfire on stream temperatures and salmonid thermal habitat in a mountain river network. Ecol Appl 2010;20(5):1350–71.
Isaak DJ, Wollrab S, Horan D, Chandler G. Climate change effects on stream and river temperatures across the Northwest U.S. from 1980–2009 and implications for salmonid fishes. Clim Chang 2012;113(2):499–524.
Labat D, Goddéris Y, Probst JL, Guyot JL. Evidence for global runoff increase related to climate warming. Adv Water Resour 2004;27(6):631–42.
Larose M, Heathman GC, Norton LD, Engel B. Hydrologic and atrazine simulation of the Cedar Creek Watershed using the SWAT model. J Environ Qual 2007;36:521–31.
Lenhart T, Eckhardt K, Fohrer N, Frede HG. Comparison of two different approaches of sensitivity analysis. Phys Chem Earth 2002;27:645–54.
Ligon F, Rich A, Rynearson G, Thornburgh D, Trush W. Report of the scientific review panel on California Forest Practice Rules and salmonid habitat. Sacramento, CA: The Resources Agency of California and the National Marine Fisheries Service; 1999.
Luo Y, Zhang X, Liu X, Ficklin D, Zhang M. Dynamic modeling of organophosphate pesticide load in surface water in the northern San Joaquin Valley watershed of California. Environ Pollut 2008;156(3):1171–81.
Luo Y, Ficklin DL, Zhang M. Approaches of soil data aggregation for hydrologic simulations. J Hydrol 2012;464-465:467–76.
Maurer EP, Wood AW, Adam JC, Lettenmaier DP, Nijssen B. A long-term hydrologically-based data set of land surface fluxes and states for the conterminous United States. J Climate 2002;15(22):3237–51.
Maurer EP, Brekke L, Pruitt T, Duffy PB. Fine-resolution climate projections enhance regional climate change impact studies. EOS Trans Am Geophys Union 2007;88(47).
McCullough DA. A review and synthesis of effects of alterations to the water temperature regime on freshwater life stages of salmonids, with special reference to chinook salmon (EPA 910-R-99-010). Washington, DC: U.S. Environmental Protection Agency; 1999.
Medlyn BE, Barton CVM, Broadmeadow MSJ, Ceulemans R, De Angelis P, Forstreuter M, et al. Stomatal conductance of forest species after long-term exposure to elevated CO2 concentration: a synthesis. New Phytol 2001;149(2):247–64.
Mohseni O, Stefan HG. Stream temperature/air temperature relationship: a physical interpretation. J Hydrol 1999;218(3–4):128–41.
Mohseni O, Stefan HG, Erickson TR. A nonlinear regression model for weekly stream temperatures. Water Resour Res 1998;34(10):2685–92.
Mohseni O, Stefan HG, Eaton JG. Global warming and potential changes in fish habitat in U.S. streams. Clim Chang 2003;59(3):389–409.
Moriasi DN, Arnold JG, Liew MWV, Bingner RL, Harmel RD, Veith TL. Model evaluation guidelines for systematic quantification of accuracy in watershed simulations. Trans ASABE 2007;50(3):885–900.
Morison JIL, editor. Intercellular CO2 concentration and stomatal response to CO2. Stomatal functionStandford University Press; 1987.
Morison JIL, Gifford RM. Stomatal sensitivity to carbon dioxide and humidity. Plant Physiol 1983;71:789–96.
Moyle PB, Katz JVE, Quiñones RM. Rapid decline of California's native inland fishes: a status assessment. Biol Conserv 2011;144(10):2414–23.
Nash JE, Sutcliffe JV. River flow forecasting through conceptual models: Part I. A discussion of principles. J Hydrol 1976;10(3):282–90.
Neitsch SL, Arnold JG, Kiniry JR, Williams JR. Soil and Water Assessment Tool, theoretical documentation, version 2009. Texas Water Resources Institute Technical Report No. 406. College Station, TX: Texas A&M University System; 2011. [http://swatmodel.tamu.edu/].
Ozaki N, Fukushima T, Harasawa H, Kojiri T, Kawashima K, Ono M. Statistical analyses on the effects of air temperature fluctuations on river water qualities. Hydrol Process 2003;17(14):2837–53.
Pan L-L, Chen S-H, Cayan D, Lin M-Y, Hart Q, Zhang M-H, et al. Influences of climate change on California and Nevada regions revealed by a high-resolution dynamical downscaling study. Clim Dyn 2011;37(9):2005–20.
Pierce D, Das T, Cayan D, Maurer E, Miller N, Bao Y, et al. Probabilistic estimates of future changes in California temperature and precipitation using statistical and dynamical downscaling. Clim Dyn 2012:1-18.
Pritchard SG, Rogers HH, Prior SA, Peterson CM. Elevated CO2 and plant structure: a review. Glob Chang Biol 1999;5:807–37.
Richter A, Kolmes SA. Maximum temperature limits for Chinook, Coho, and Chum Salmon, and Steelhead Trout in the Pacific Northwest. Rev Fish Sci 2005;13(1): 23–49.
Runkel RL, Crawford CG, Cohn TA. Load Estimator (LOADEST): a FORTRAN program for estimating constituent loads in streams and rivers: U.S. Geological Survey Techniques and Methods Book 4; 2004 [Chapter A5, 69 pp.].
Sharpley AN, Williams JR. EPIC—Erosion/Productivity Impact Calculator: 1. Model Documentation. US Department of Agriculture, Technical Bulletin No. 1768. Washington, DC: US Government Printing Office; 1990.
Stefan HG, Preud'homme EB. Stream temperature estimation from air temperature. J Am Water Resour Assoc 1993;29(1):27–45.
Stockle CO, Williams JR, Rosenberg NJ, Jones CA. A method for estimating the direct and climatic effects of rising atmospheric carbon dioxide on growth and yield of crops: Part I—Modification of the EPIC model for climate change analysis. Agr Syst 1992;38(3):225–38.
USEPA. EPA Region 10 Guidance for Pacific Northwest State and Tribal Temperature Water Quality Standards (EPA 910-B-03-002). Washington, DC: U.S. Environmental Protection Agency, Region 10 Office of Water; 2003.
USEPA. Data for the Better Assessment Science Integrating Point and Nonpoint Sources (BASINS) model. Washington, DC: U.S. Environmental Protection Agency; 2007 [http://www.epa.gov/waterscience/ftp/basins/gis_data/huc/, accessed 05/2012].
USEPA. Integrated reporting categories 303(d) submission. Washington, DC: U.S. Environmental Protection Agency; 2011 [http://www.epa.gov/waterscience/standards/academy/supp/tmdl/page7.htm, accessed 04/2011].
Van Liew MW, Garbrecht J. Hydrologic simulation of the Little Washita river experimental watershed using SWAT. J Am Water Resour Assoc 2003;39(2):413–26.
van Vliet MTH, Ludwig F, Zwolsman JJG, Weedon GP, Kabat P. Global river temperatures and sensitivity to atmospheric warming and changes in river flow. Water Resour Res 2011;47(2):W02544.
Wand SJE, Midgley GF, Jones MH, Curtis PS. Responses of wild C4 and C3 grass (Poaceae) species to elevated atmospheric CO2 concentration: a meta-analytical test of current theories and perceptions. Glob Chang Biol 1999;5:723–41.
Webb BW, Clack PD, Walling DE. Water–air temperature relationships in a Devon river system and the role of flow. Hydrol Process 2003;17(15):3069–84.
Webb BW, Hannah DM, Moore RD, Brown LE, Nobilis F. Recent advances in stream and river temperature research. Hydrol Process 2008;22(7):902–18.
Winchell M, Srinivasan R, Di Luzio M. and Arnold J. ArcSWAT interface for SWAT2009, user's guide (http://swatmodel.tamu.edu/software/arcswat/). Blackland Research Center, Texas Agriculutral Experiment Station, Temple, TX; Grassland, Soil and Water Research Laboratory, USDA Agriculutral Research Service, Temple, TX, 2011.
Wood AW, Maurer EP, Kumar A, Lettenmaier DP. Long-range experimental hydrologic forecasting for the eastern United States. J Geophys Res 2002;107(D20):4429.
Wood AW, Leung LR, Sridhar V, Lettenmaier DP. Hydrologic implications of dynamical and statistical approaches to downscaling climate model outputs. Clim Chang 2004;62(1):189–216.
Wu Y, Liu S, Abdul-Aziz O. Hydrological effects of the increased CO2 and climate change in the Upper Mississippi River Basin using a modified SWAT. Clim Chang 2012;110(3): 977-1003.
Young CA, Escobar-Arias MI, Fernandes M, Joyce B, Kiparsky M, Mount JF, et al. Modeling the hydrology of climate change in California's Sierra Nevada for subwatershed scale adaptation. J Am Water Resour Assoc 2009;45(6):1409–23.